České vysoké učení technické v Praze
Czech Technical University in Prague

Fakulta jaderná a fyzikálně inženýrská
Faculty of Nuclear Sciences and Physical Engineering

Ing. Václav Čuba, Ph.D.

Radiační příprava anorganických sloučenin
Radiation preparation of inorganic compounds

Summary

Radiation methods present powerful tool for synthesis of various inorganic materials. Study of solid particles formation from solutions in the field of UV or ionizing radiation is one of the very promising and long term pursued trends in photochemistry and radiation chemistry. The motivation may be various, either preparation of new materials or removal of hazardous contaminants (e.g. heavy metals) from wastewater. This lecture deals with preparation of metals, metal oxides and garnets via irradiation of aqueous solutions containing precursors. Namely, radiation induced preparation of metallic silver and copper is explored, as well as preparation of cuprous, zinc, nickel, yttrium and aluminium oxide and yttrium aluminium garnet. As the sources of radiation, medium pressure UV lamp, ^{60}Co irradiator and linear electron accelerator were used. Aside from preparation, various physico-chemical and structural properties of prepared compounds are discussed.

Souhrn

Radiační metody představují účinný nástroj pro syntézu nejrůznějších anorganických sloučenin. Studium vzniku tuhé fáze z roztoku v poli UV nebo ionizujícího záření patří k velice slibným a dlouhodobě studovaným oblastem fotochemie a radiační chemie. Důvodem pro toto studium přitom nemusí být jen příprava nových materiálů, ale také odstranění nebezpečných kontaminantů (např. těžkých kovů) z vod. Náplní této přednášky je příprava kovů, kovových oxidů a granátů ozařováním vodných roztoků jejich prekurzorů. V přednášce je popsána radiačně indukovaná příprava kovového stříbra a mědi, oxidů měďného, zinečnatého, nikelnatého, yttritého a hlinitého a granátu yttrito – hlinitého. Jako zdroje záření byly použity střednětlaká rtuťová výbojka, radionuklidový ^{60}Co ozařovač, a lineární urychlovač elektronů. Kromě přípravy jsou diskutovány také různé fyzikálně chemické a strukturní vlastnosti připravených sloučenin.

Klíčová slova

Ionizující záření, UV záření, radiační syntéza, nanočástice, optické materiály, katalyzátory, kovy, kovové oxidy, syntetické granáty

Keywords

ionizing radiation, UV radiation, radiation synthesis, nanoparticles, optical materials, catalysts, metals, metal oxides, synthetic garnets

Obsah

1. Introduction

The synthesis of various inorganic compounds using ionizing radiation (IR) or UV light represents one of my main research interests. Radiation processes have some advantages over common chemical methods: they are mostly independent of temperature and they yield material of high purity, with narrow size distribution of particles. Radiation technique is rather simple method for preparation of various compounds. It is based on irradiation of aqueous solutions containing suitable precursors with ionizing or UV radiation. Finely dispersed solid phase formed during irradiation is subsequently separated from solution, dried and either used as is, or further processed by calcinating at high temperatures under various atmospheres. The preparation enables fast production of good amounts of powder materials. Moreover, no strict control of experimental conditions is required. Currently, the method has been successfully tested for preparation of wide array of nano-scale compounds, namely metals, metal oxides, garnets and spinels.

Materials consisting of nanometre-sized particles have drawn substantial attention in wide range of research fields, mostly for their various unique properties originating from their small size or related high specific surface area. For this reason, the nanoscale materials are considered for many applications (e.g. as catalysts or scintillators).

The lecture deals with radiation preparation of silver and copper metallic particles, cuprous, zinc, nickel, aluminium and yttrium oxides, and yttrium aluminium garnet.

2. Principle of the method

Both ionizing and non-ionizing radiations present powerful tools for synthesis or processing of various materials. For preparation of materials from aqueous solution using ionizing radiation, the radiolysis of water plays important role. It results in formation of reactive intermediates, summarized as (Buxton et al. 1988):

$$H_2O + h\nu \rightarrow e^-_{aq}, H, OH, H_2, H_2O_2, H^+ .$$

Preparation using non-ionizing UV radiation or visible light encompasses:

- usage of sensitizers (e.g. benzophenone or methylene blue), which produce radicals upon irradiation, reacting with target compound (Kapoor et al. 2002; An et al. 2001);
- direct photolysis of studied compounds, which results in formation of desired material (Loginov et al. 2002; Giuffrida et al. 2008);
- reactions with products of water photolysis (Mallick et al. 2004; Azrague et al. 2005). Although the direct photolysis of water occurs at wavelengths longer than 200 nm, it becomes more significant at wavelengths of UV radiation shorter than 200 nm (Azrague et al. 2005). The main products of photolysis are OH radical and hydrogen radical (quantum yield of hydrated electron is lower than 0.05):

$$H_2O + h\nu \rightarrow H_2O^* \rightarrow OH + H\ .$$

Subsequently, hydrogen peroxide may be formed due to mutual reaction of two OH radicals, similarly to radiolysis.

Metal ions present in irradiated solutions may be reduced to lower valences via their reactions with reducing radicals coming from radiolysis of water or dissolved compounds, e.g.:

$$M^{n+} + e^-_{aq} \rightarrow M^{(n-1)+}\ ;$$

$$M^{n+} + H \rightarrow M^{(n-1)+} + H^+\ ;$$

$$M^{n+} + (CH_3)_2COH \rightarrow [M(CH_3)_2COH]^{n+} \rightarrow M^{(n-1)+} + H^+ + (CH_3)_2CO\ ;$$

$$M^{n+} + COO^- \rightarrow [MCOO]^{(n-1)+} \rightarrow M^{(n-1)+} + CO_2\ .$$

Disproportionation of partially reduced states is another mechanism for transition of metal ions to lower valences, e.g.:

$2Au^{2+}Cl_3^{1-} \rightarrow Au^{1+}Cl_2^{1-} + Au^{3+}Cl_4^{1-}$.

Atoms of metals or partially reduced ions may agglomerate to form clusters (Belloni et al. 1998):

$$M^0 + M^0 \rightarrow M_2;\ M^0 + M^+ \rightarrow M_2^+\ .$$

Agglomeration and reduction of ions adsorbed on surface of clusters results, in the end, in formation of metallic suspended matter. To retain colloidal properties of metal clusters, nanoparticle stabilizers, preventing excessive agglomeration, must be added in solution.

There are basically few possible mechanisms of oxide particles formation; one of them is partial or total radiation reduction of dissolved metal ions to metallic particles via reactions with hydrated electrons, followed by their oxidation via reaction with oxygen under suitable conditions:

$$2Me + O_2 \rightarrow 2MeO.$$

The formation of metallic oxides in the field of radiation may also occur due to partial reduction of metal ions, followed by reaction with hydroxyl ions

$$2Me^+ + 2OH^- \rightarrow 2Me(OH) \rightarrow Me_2O + H_2O,$$

or by disproportionation

$$2Me^+ \rightarrow Me^0 + Me^{2+}.$$

Another possibility is radiation induced formation of amorphous solid phase, which may be subsequently calcinated to form required crystalline compound. This method is often utilized for preparation of more complicated structures, such as garnets and spinels.

In the last decades, radiation or photochemical reduction was successfully utilized for preparation of small-sized particles or composite clusters consisting of one or more metals. Both noble and non-noble metals were successfully reduced to form nanocolloids, predominantly copper (Kumar et al. 1999; Zhou et al. 2008), silver (Mallick et al. 2004; Shvalagin et al. 2004, 2007), platinum or nickel (Belloni et al. 1998). Similarly, cuprous and zinc oxides were prepared from aqueous solutions in recent years, using UV (Buono-Core et al. 2006; Tak and Yong 2008) or ionizing (Zhu et al. 1994; Rath et al. 2009) radiation. Recently, direct photochemical preparation of zinc peroxide was also reported

(Sun et al. 2007; Sebok et al. 2009). This compound was prepared by irradiation of aqueous solution containing zinc acetate and hydrogen peroxide using 35 or 75W Xe lamp:

$$Zn(CH_3COO_2)_2 + H_2O_2 \xrightarrow{h\nu} ZnO_2 + 2CH_3COOH\,.$$

Nevertheless, the papers dealing with radiation preparation of metal oxides are still rather scarce and no reports dealing with radiation preparation of nickel, yttrium and aluminium oxides or garnets have been published, yet.

3. Experimental background

All used chemicals were of analytical grade purity or better. Deionized water was used for the preparation of all solutions. Various metal salts were used as precursors. Concentrations of precursors in irradiated solutions generally ranged from 10^{-3} to $5x10^{-2}$ mol dm^{-3}. Other compounds were added to solutions, fulfilling roles of radical scavengers (propan-2-ol, potassium formate), macromolecular stabilizers (polyvinyl alcohol - PVA) or sources of oxidizing species (hydrogen peroxide) during radiolysis. No further additives affecting the natural pH of solutions were used. When necessary (i.e. for silver and copper particles preparation), some studied solutions were purged by nitrogen gas prior to irradiation.

High energy electron irradiation was performed on linear electron accelerator LINAC 4-1200 (Tesla v.t. Mikroel), with electron energy 4.5 MeV, pulse width 3 μs and repeating frequency 500 Hz. In each experiment, 1-2 dm^3 of various solutions were irradiated in thin layer (1cm) on glass Petri dishes or in sealed polypropylene flasks. The ^{60}Co in Gammacell 220, company Nordion, was used for gamma irradiation ($E_{\gamma1}$ = 1.23 MeV; $E_{\gamma2}$ = 1.39 MeV). The samples were irradiated exclusively in sealed polypropylene flasks. Doses were determined using the Fricke dosimeter. Applied doses of both types of ionizing radiation ranged from units to hundreds of kGy.

UV-VIS irradiation was mostly performed using medium pressure mercury lamp UVH 1016-6 (UV Technik Meyer GmbH) with variable power input 140-400 W, emitting photons at wavelengths 200-580 nm (70% of emitted intensity in UV area 200-400 nm). The lamp in quartz tube was immersed in 2 dm^3 of solutions in glass reactor with thermometer. During irradiation, the solutions were continually stirred and the reactor was cooled with water, so that the temperature of irradiated solution did not exceed 45°C. Potassium ferrioxalate actinometry was performed under the same conditions. Irradiation generally took tens of minutes at photon flux $2\text{-}5x10^{19}$ $h\nu\ s^{-1}$. The low pressure mercury lamp (6 W, Photochemical reactors, Ltd, Sylvania) emitting the radiation with the wave length of 254 nm was used for some experiments. In this case, the photon flux ($7\ 10^{17}$ $h\nu\ s^{-1}$) was measured by iodide-iodate actinometer.

Visual MINTEQ software (version 3.0) was used for calculating speciation of prepared solutions. The pH of irradiated solutions was measured using pH/conductivity meter Jennway 3540. The absorption spectra were measured using spectrophotometer Carry 100 in the range 190 – 900 nm. After irradiation, the formed finely dispersed solid phase was separated in glove-box via Amicon nitrogen-pressurized microfiltration (Millipore HAWP 0.45 μm), washed with water and ethanol, and dried at 40°C to the constant weight. When necessary, the samples were thermally treated for various time (usually 1-2 hours at various temperatures in air, nitrogen or vacuum using Clasic 0415VAK oven (heating rate 5-15°C min^{-1}).

The solid phase was characterized via x-ray powder diffraction (XRPD), using modified HZG-3 diffractometer (RTG lamp with copper anode; weighted average wavelength $K_{\alpha 1,2}$ of the copper 0.15418 nm) with scintillation detector. ICDD PDF-2 database was used for identification of prepared crystalline materials. Thermal analysis - mass spectroscopic technique (TA-MS, Netzsch STA (QMS) 409/429-403) and high resolution transmission electron microscopy (HRTEM, JEOL 3010) were used as additional methods for solid phase characterization.

Specific surface area (SSA) of prepared solid materials was determined using selective sorption of nitrogen gas from catalytically deoxygenated mixture of 5 H_2 : 1 N_2 at the temperature of 77 K. The deficiency of nitrogen in the gas due to sorption on solid sample was detected by thermal conductivity detector and recorded in computer. Specific surface area was then calculated by relating the area of desorption peak from sample to desorption peak from TiO_2 standard (48.88 $m^2.g^{-1}$, measured by BET).

To evaluate scintillation spectra of some prepared materials (ZnO, YAG), radioluminescence measurements under excitation by X-ray tube (Seifert, 40 kV, 15 mA) were performed, using custom made 5000M fluorometer (Horiba Jobin Yvon).

Catalytic activity of prepared Cu_2O and NiO powders was studied by measuring the rate of oxygen formation during catalytic decomposition of 1.2 mol.dm^{-3} solution of hydrogen peroxide H_2O_2 in thermostated reactor at several temperatures.

4. Silver

Silver ions are easily reduced in solutions via UV or IR to form colloids. Thus, nanostructures of metallic silver are very convenient to study. Silver nitrate and silver cyanide were used as precursors for radiation and/or photochemical reduction of Ag^+ ions to the metallic form. Citric acid, propan-2-ol and PVA were used as scavengers and stabilizer.

Under given conditions, gamma irradiation initiates formation of colloidal nanoparticles at doses around 1kGy. In some systems, true colloid form (yellow colour) is very non-stable and shifts rather quickly into aggregated (dark violet or black) form, which eventually sediments in the bottom of vessel. This is in full agreement with presumption, that two opposing mechanisms take place in the system. First, nucleation of silver atoms reduced by ionizing radiation is initiated. Second, radiation may start to dissolve solvatation shell of growing colloid particles and disrupt charge equilibrium on their surface (Nikonorova et al., 1976). Thus, small particles start to aggregate to bigger clusters, which eventually deposit in the bottom of the vials. Performed experiments showed that stabilizer is needed for control of kinetics of nucleation. In solutions containing PVA, the reduced silver retained its colloidal properties even at the dose 10 kGy.

Estimated size of prepared silver particles, drawn from RTG diffractograms and from comparison of obtained UV/Vis spectra shapes with theoretically calculated spectra for particles of various size (Sukhov et al., 1997), ranges from 30 to 40 nm.

Comparison of ionizing and UV irradiation shows very similar behavior of all studied solutions. UV treatment leads to rather quick formation of black aggregated nanoparticles in non-stabilized solutions, probably due to high flow of photons and good photosensitivity of solutions containing silver. UV irradiation of solutions with stabilizing PVA leads to formation of stable colloid form.

RTG diffraction analysis showed in all cases predominant presence of silver. Small amount of silver oxide was also detected, probably due to reaction of silver with atmospheric oxygen during samples preparation and measurement.

Following comments can be made based on obtained data:

Ionising and UV radiation have been successfully utilized for preparation of silver nanopowder from solutions containing inorganic precursors. No significant differences in the characteristics of products formed under both types of radiation were found. Deoxygenation and presence of OH radical scavenger are necessary for radiation reduction to occur. Without added stabilizer, colloid particles tend to aggregate and form solid sediments at higher doses of radiation.

5. Copper and cuprous oxide

Similarly to silver, copper nanoparticles may be easily obtained from aqueous solutions via radiation reduction. Copper may oxidize to form stable oxides. Nanoparticles of cuprous oxide are often studied, because this oxide is well known semiconductor, catalyst and photocatalyst. In this work, copper sulphate pentahydrate or copper formate hydrate were used as precursors for Cu or Cu_2O preparation; additionally, hydrogen peroxide, propan-2-ol and/or PVA were added to irradiated solutions. Commercial cuprous oxide was used for comparison of its catalytic properties with our prepared materials.

Nanometre-sized spherical Cu and octahedral Cu_2O catalysts were successfully synthesized by radiation- or photo-induced reduction of Cu^{2+} aqueous solutions and several parameters influencing their formation and stability have been studied. Cuprous oxide was not formed by oxidation of metallic copper by oxygen but originated from spontaneous decay of yellow-coloured unstable cuprous hydroxide CuOH. Black colour of prepared cuprous oxide (as opposed to red colour of bulk Cu_2O) may be caused either by thin cupric oxide layer on the surface of particles or by their small dimensions. According to our observations, radiation- and photo-induced reduction of studied solutions has lead to equivalent changes of absorption spectrum with dose / irradiation time and identical solid phase composition.

Obtained results do not indicate any differences in absorption spectra or formed solid phase composition between aerated solutions and solutions purged by nitrogen except for the dose required to achieve the same effect (which is higher in aerated solutions). This difference may be attributed to the dose needed for consumption of dissolved oxygen in aerated solutions. Product composition seems to be influenced by pH and also by actual concentration of reducible copper species; both values naturally decrease during the reduction process. At 10^{-2} mol.dm^{-3} precursor concentration and low dose, pure cuprous oxide may be formed, whereas at 10^{-3} mol.dm^{-3} only copper is produced. As far as I know, this strong dependence on concentration has not yet been reported in literature.

Electron microscopy revealed that in case of pure copper the particles are relatively large (diameter up to about 400 nm), of spherical shape and heavily agglomerated. Pure cuprous oxide samples, however, contain rather angled shapes, mostly symmetrical octahedra up to 300 nm in diameter as can be seen in Fig. 1. SAED pattern of the octahedron depicted in Fig. 1 clearly indicates that prepared powder consists of monocrystalline particles as no diffraction rings are present.

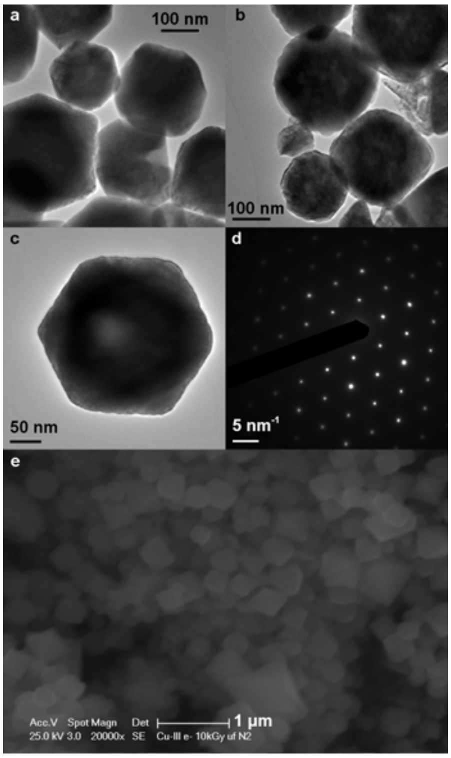

Figure 1: a), (b) - HRTEM images of separated Cu_2O powder from N_2 purged 10^{-2} mol.dm^{-3} $Cu(HCOO)_2$ + propan-2-ol + PVA solution irradiated by electron beam with dose 10 kGy; (c) - Cu_2O octahedron in the same sample and (d) - its SAED pattern; (e) - SEM image.

The majority of prepared solid materials has relatively low SSA of approximately 3.0 m^2.g^{-1} (Tab. 1). Surface-normalised catalytic activity of prepared Cu_2O powder towards decomposition of hydrogen peroxide was found to be comparable to commercial cuprous oxide. Non-normalised catalytic activity is, however, about four times greater than for commercial Cu_2O.

Performed experiments shown that photo- or radiation-induced reduction of copper(II) salts in aqueous solutions can be used for convenient preparation of pure nanocrystalline copper or cuprous oxide catalysts at normal temperature only by adjusting the dose and copper(II) concentration.

material description		*SSA* [$m^2.g^{-1}$]	k_s [$mol.m.s^{-1}$]		
			30 °C	35 °C	40 °C
commercial Cu_2O		0.51	1.64	2.03	2.72
$Cu(HCOO)_2$, 10 kGy, N_2 purged		2.78	0.69	1.07	1.81
$Cu(HCOO)_2$ + propan-2-ol, 10 kGy, N_2 purged		3.09	0.87	1.26	2.22
$Cu(HCOO)_2$ UV, purged by N_2	untreated	2.81	0.86	1.20	2.00
	vacuum, 200 °C	2.93	0.90	1.13	1.87
	air, 200 °C	3.37	0.70	0.88	1.45
$Cu(HCOO)_2$ UV, unpurged	untreated	2.32	0.77	1.17	2.11
	vacuum, 200 °C	3.32	0.61	0.93	1.68
	air, 200 °C	3.09	0.93	1.17	1.84

Table 1: measurement results for specific surface area and catalytic activity of prepared Cu_2O samples.

6. Zinc oxide

Zinc oxide, commonly occurring as hexagonal wurtzite, is the n-type semiconductor with large direct band gap (~ 3.4 eV) and large exciton binding energy 60 meV. It has been intensively studied due to its piezoelectric, pyroelectric, photocatalytic and conductive properties and it has currently wide range of possible applications, including acoustic wave devices, optical waveguides, LED diods, solar cells, chemical sensors or photovoltaic devices. Moreover, exciton luminescence of zinc oxide is conveniently placed at the border of ultraviolet and visible areas, around 395 nm. It has sub-nanosecond lifetime (Wilkinson et al. 2004), which makes it suitable for possible application in fast scintillating materials. Scintillation efficiency is noticeably increased when ZnO is doped with donor ions, such as Ga^{3+} and when targeted annealing procedures are applied to the prepared powders (Bourret-Courchesne et al. 2009).

As in previous cases, comparative study dealing with characterization of zinc oxide prepared from various precursors under ionizing or non-ionizing radiation was performed. It revealed many similarities between materials prepared under both types of irradiation. Zinc nitrate or formate was used as precursor for zinc oxide preparation. Similarly to previous chapters, propan-2-ol and PVA were used, too. Additionally, hydrogen peroxide (source of oxidative species) was added to some solutions.

Evaluation of pH and absorption spectra of irradiated solutions reveals no noticeable difference between ionizing and non-ionizing radiation. Typically, pH increases during irradiation up to value ~ 6. The absorption of irradiated solutions monotonously increases with irradiation time due to increasing amount of formed solid phase.

Comparison of XRPD spectra of all discussed materials is shown in Fig. 2. Regardless of the type of irradiation the solid phase obtained from solutions consists of hexagonal zinc oxide and possibly also of rare tetragonal volume-centered zinc oxide. In some cases, pure crystalline zinc peroxide was detected. It was confirmed that at higher temperatures, well developed zinc oxide (hexagonal) crystalline nanoparticles are formed, regardless of the irradiation type or initial precursors.

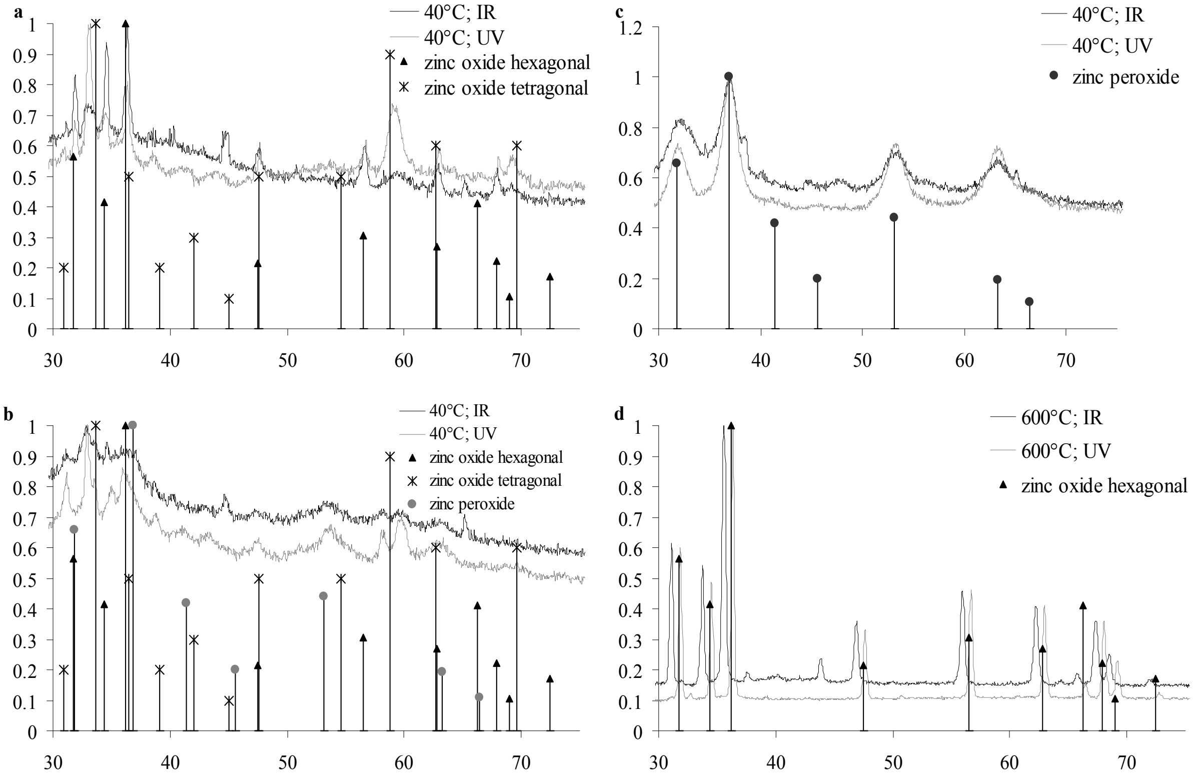

Figure 2:comparison of solid materials prepared from various precursors under ionizing or UV irradiation; a – zinc nitrate and propan-2-ol; b – zinc formate and PVA; c – zinc formate, PVA and hydrogen peroxide; d – solid phase from any solution.

TEM/SAED images showed that prepared material is polycrystalline. This was observed in all studied systems, contrary to work of other authors (Hu et al. 2005), who irradiated micellar solutions and obtained single crystalline material. SEM images of ZnO formed under either of both types of radiation show regularly shaped rice-like structures with size around 100 nm (examples in Fig. 3).

The size of the particles and specific surface area of solid phase depend strongly on calcination temperature and varies somewhat between materials, but it does not seem to depend too much on the type of used radiation (Tab. 2).

From the luminescence intensity point of view, the calcination conditions, namely temperature and atmosphere, are more important than the precursors for material preparation. Generally, the higher temperature, the higher luminescence intensity was observed, most probably due to thermal decomposition of impurity phases, changes in stoichiometry and/or point defect characteristics of zinc oxide particles. All samples calcinated at temperatures higher than 650°C showed under X-ray excitation the intensive visible luminescence, when compared with the standard $Bi_4Ge_3O_{12}$ (BGO) scintillator sample as for the absolute intensity. Moreover, our samples showed well-shaped exciton luminescence at 390-400 nm, belonging to emission of (phonon replica of) free exciton.

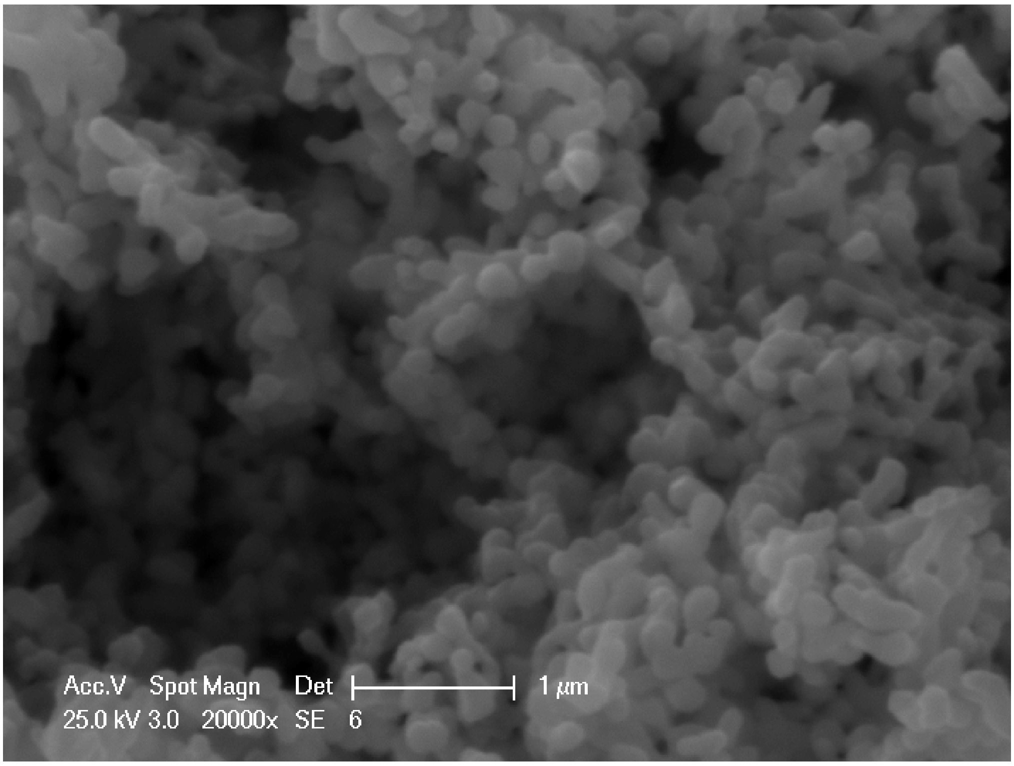

Figure 3: SEM image of nanocrystalline ZnO prepared by UV irradiation of solution containing zinc nitrate and propan-2-ol and calcinated at 600°C.

Solid phase from solution containing zinc nitrate and propan-2-ol			
Temperature [ºC]	SSA [m^2 g^{-1}]*	Diameter [nm]*	Diameter [nm]**
40	75	7.1	28
650	11	48.6	168
1000	2.5	214	224
Solid phase from solution containing zinc formate and PVA			
Temperature [ºC]	SSA [m^2 g^{-1}]*	Diameter [nm]*	Diameter [nm]**
40	5.4	99	N/A
650	3	178	232
1000	2.4	223	250
Solid phase from solution containing zinc formate, PVA and hydrogen peroxide			
Temperature [ºC]	SSA [m^2 g^{-1}]*	Diameter [nm]*	Diameter [nm]**
40	136	3.9	N/A
650	3.2	167	112
1000	27.5	20	25

* *- values obtained for materials prepared under UV irradiation*

** *- values obtained for materials prepared under ionizing irradiation*

Table 2: specific surface area and particle size of ZnO prepared under ionizing and UV radiation from various precursors.

Radioluminescence spectra of these samples are qualitatively similar to the spectrum of single crystal of ZnO - hydrothermally grown sample in Tokyo Denpa (Ohshima et al. 2004), which confirms the purity and quality of prepared material (Fig. 4a). Fig. 4b shows the radioluminescence spectra of identical samples, but prepared under UV irradiation and calcinated at 1000ºC in air. The shapes of the spectra are practically identical.

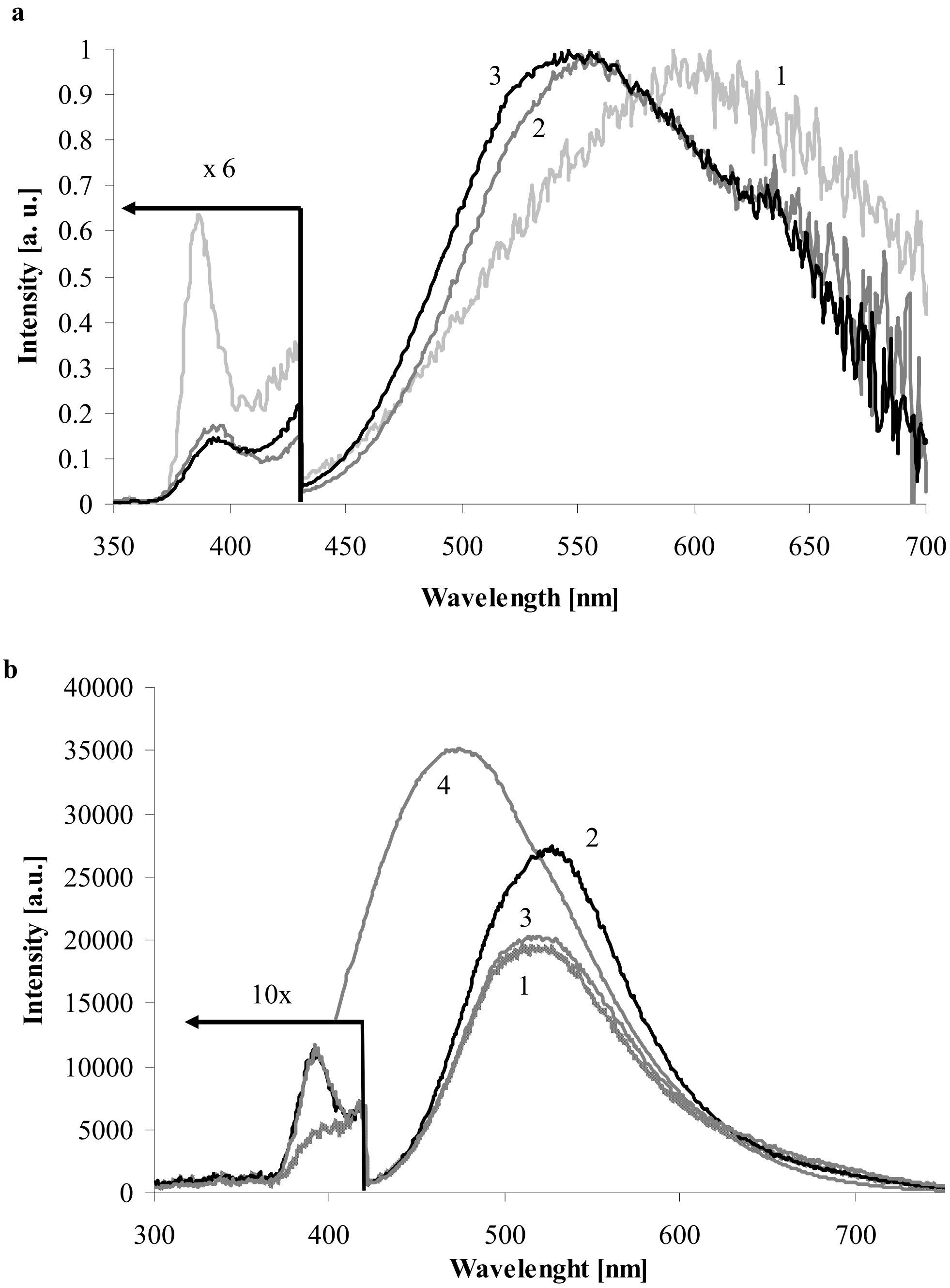

Figure 4: room-temperature radioluminescence spectra; a – comparison of ZnO nanopowders prepared by accelerated electrons irradiation and calcinated at 1000°C with ZnO bulk single crystal (1); b – same materials prepared under UV irradiation (1, 2, 3), compared to BGO/10 (4).

Recently, the doping of zinc oxide with Ga has been used to enhance scintillation efficiency of ZnO (Bourret-Courchesne et al. 2009). The method for further increasing the excitonic luminescence of zinc oxide doped with gallium, based on treating the samples for 0.5 h at 800°C in the stream of H_2/Ar mixture (1:20), was used with good results.

Based on these results, the lanthanum or galium doped samples were prepared by UV irradiation of aqueous solutions. Lanthanum acetate or galium nitrate were added to the solutions prior irradiation, so that their concentration varied between 100-500 ppm. When compared to Ga^{3+}, significantly higher local lattice distortion can be expected in the case of La^{3+} due to its much bigger radius. Both the visible and UV luminescence of ZnO is significantly increased by presence of both ions. Furthermore, the effect of a post-growth annealing treatment in reductive H_2-containing atmosphere was studied following the description given by Bourret-Courchesne et al. (2009), see example in Fig. 5. Consistently with the results reported in this reference, the significant increase of the excitonic UV emission in both undoped and Ga/La-doped samples was observed.

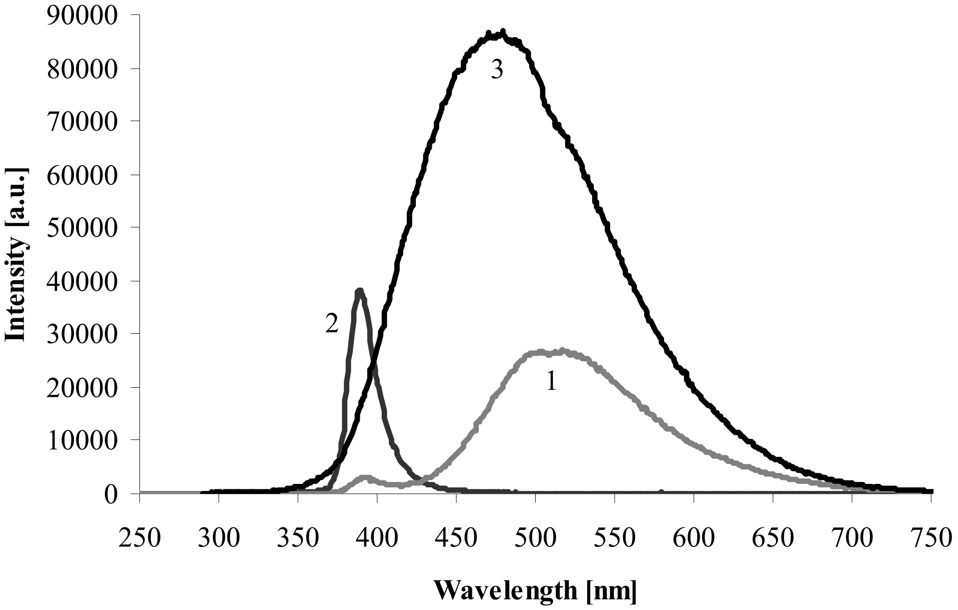

Figure 5: room-temperature radioluminescence spectra; 1 - ZnO doped with 100 ppm Ga; 2 – the same sample, but with additional treatment in Ar/H_2 at 800°C; 3 – BGO standard.

7. Nickel oxide

Nickel oxide is the p-type semiconductor with octahedral crystalline structure. It occurs either as stoichiometric green or non-stoichiometric black compound with abundant oxygen. Applications of nickel oxide are based on its semiconductive, magnetic and optical properties. It is widely used as a catalyst of redox reactions or as a precursor for preparation of nickel-based catalysts, as a main component in gas sensing elements, solar cells, in chemical fuel rods, electrodes in various electrical and optoelectronic facilities, electrical ceramic components such as thermistors, varistors and glass or ceramic pigments.

As in previous cases, UV light, ^{60}Co gamma and accelerated electrons were successfully used for preparation of crystalline nickel oxide; aqueous solutions containing nickel formate alone or in mixture with isopropyl alcohol were irradiated. The pH of prepared solutions was neutral; no significant pH changes were observed during irradiation. Under all types of irradiation, weakly crystalline solid phase is formed; pure nickel oxide phase was found at temperatures as low as 300°C in air. XRPD spectra of samples formed under electron and UV radiation and thermally treated under various conditions were evaluated. The lowest temperature of crystalline NiO formation was determined to be 300°C. Similarly to zinc oxide, the thermal treatment of all samples at 600 °C in air resulted in formation of nickel oxide with well-developed crystals, regardless of the type of initial solution and irradiation.

Values of linear crystallite size *l* of nickel oxide, calculated from XRPD spectra, mostly range between 20-25 nm. The values are very similar for all materials, except for NiO prepared from solution containing both nickel formate and propan-2-ol by UV irradiation (10 nm). Possibly, the combination of UV irradiation and presence of propan-2-ol in irradiated solution leads to higher rate of crystallization and, consequently, to smaller linear crystallite size of NiO.

Values of SSA are shown in Tab. 3. It is interesting to note, that the SSA of samples dried at room temperature reach, regardless of the kind of irradiation, the similar values. In most cases, SSA increased after heat treatment at 200°C (probably due to metallic nickel formation). The samples annealed at 200°C in vacuum show lower SSA values than samples annealed at 200°C in air. Possibly, an over-stoichiometric surface oxygen plays a role here. The higher temperature (600°C) of annealing, at which NiO with well developed crystals was invariably formed, results in some cases in slight decrease of SSA, probably due to the sintering of material.

Sample (irradiation)	***SSA*** [m^2 g^{-1}]	**Sample (irradiation)**	***SSA*** [m^2 g^{-1}]
nickel formate (e-)		**nickel formate + propan-2-ol (e-)**	
untreated	10.9	untreated	15.9
Air, 200°C	20.3	Air, 200°C	14.3
Vacuum, 200°C	12.3	Vacuum, 200°C	4.7
Vacuum, 600°C	9.3	Vacuum, 600°C	9.0
nickel formate (UV)		**nickel formate + propan-2-ol (UV)**	
untreated	6.4	untreated	27.8
Vacuum, 200°C	115.1	Vacuum, 200°C	77.6
Vacuum, 600°C	89.2	Vacuum, 600°C	87.3
nickel formate (γ)		**NiO_{std}**	4.6
untreated	18.3		
Vacuum, 200°C	55.8		
Vacuum, 600°C	20.1		

Table 3: specific surface area of prepared NiO powders compared to nickel oxide standard.

The SSA of all samples prepared under ionizing or UV irradiation was found to be several times higher than the SSA of NiO standard. SSA values of nickel oxide prepared under UV irradiation are rather high, reaching values up to ~100 $m^2\ g^{-1}$ (exceeding NiO standard roughly 20 times), while SSA values of materials prepared under electron irradiation do not exceed 20 $m^2\ g^{-1}$. When compared to the UV or gamma irradiation, the deposition of energy under accelerated electrons irradiation is very fast and highly non-uniform. Linear electron accelerator implants the energy to the matter in short pulses (~ 3 μs), followed by comparatively long relaxation time (2 ms), which may affect physico-chemical parameters of prepared material, including SSA values.

HRTEM and SAED images confirm high porosity and polycrystallinity of prepared nickel oxide (without preferential orientation) regardless of the type of irradiation (Fig 6).

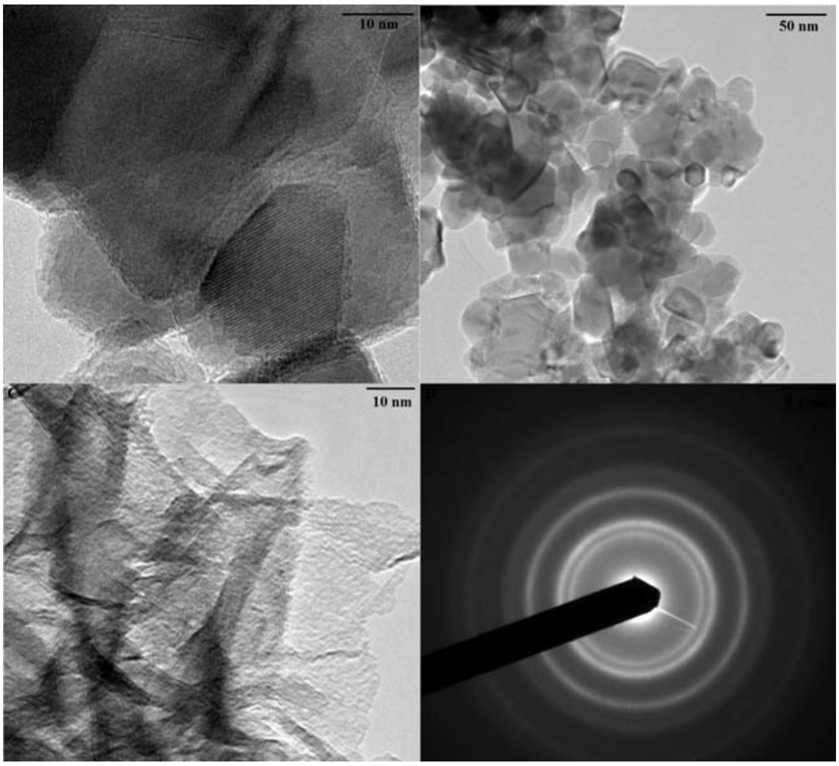

Figure 6: upper left and right - HRTEM images of NiO calcinated under vacuum at 600°C; lower left and right – HRTEM and SAED images of solid phase separated from solution after UV-irradiation and dried at room temperature.

Under given conditions, UV irradiation seems to be best suited for preparation of nickel oxide; it yields material with high porosity, large specific surface area, and, therefore, high catalytic activity, tested on hydrogen peroxide decomposition.

8. Yttrium oxide

Powder yttrium oxide is white crystalline material with cubic structure. Porous Y_2O_3 with high surface area is used as selective catalyst for various reactions. Pure or doped Y_2O_3 is used for the manufacture of phosphors and ceramics. Europium activated yttrium oxide is a well-known red emitting phosphor used in lightening industry and optoelectronic devices; cerium (III) doped yttrium oxide is promising scintillator; gadolonium-doped yttrium oxide is potentially useful as an ultraviolet source, since ultraviolet light is emitted when electron transition between energy states in Gd ions occurs; neodymium-activated yttrium oxide optical ceramics is usable for active media of solid-state lasers. Moreover, powder Y_2O_3 is and important precursor for pure or doped (powder) YAG preparation, namely via solid state reactions, sol-gel and coprecipitation methods.

Photochemical/radiation technique presents an easy alternative method for yttrium oxide preparation. However, similarly to other techniques, it requires consequent thermal treatment to obtain material with good crystallinity. For radiation experiments, yttrium nitrate hexahydrate, potassium formate and propan-2-ol were used. Calcination at temperatures in the interval ~ 450 - 1200°C interval is usually utilized for obtaining crystalline Y_2O_3 particles (Huang et al. 2006; Muresan et al. 2009). In our studied systems, diffraction lines of yttrium oxide with well developed crystals were found after annealing for 1 hour at 600°C. Calculated crystallite size of the samples annealed at 600 – 1200°C reaches tens of nm. It generally increases with temperature due to aggregation. Particle size of materials annealed at 600°C is similar for all solutions and irradiation types, though at higher annealing temperatures when agglomeration of nanoparticles and recrystallization of material occurs, the particle size starts to vary considerably. At all annealing temperatures, the smallest particles were observed at materials prepared under electron irradiation, while the materials prepared under UV irradiation with maximum power output consist of bigger particles.

Specific surface area of samples annealed at 600°C reaches values up to 40 $m^2\ g^{-1}$ and was observed to decrease at higher calcination temperatures, which is due to sintration effects of the surface. This value is quite high, as various methods of porous Y_2O_3 preparation lead to SSA values in the range 10 – 65 $m^2\ g^{-1}$.

SEM images show that during irradiation, particles with uniform, roughly spherical shapes (rice-like) are formed. The shape corresponds to materials prepared by other authors (Muresan et al. 2009). HRTEM images (Fig. 7) show, that the material calcinated at 600°C and higher consists of cubic monocrystals with ~ 50 nm size. The monocrystalline character of material was confirmed by SAED measurement.

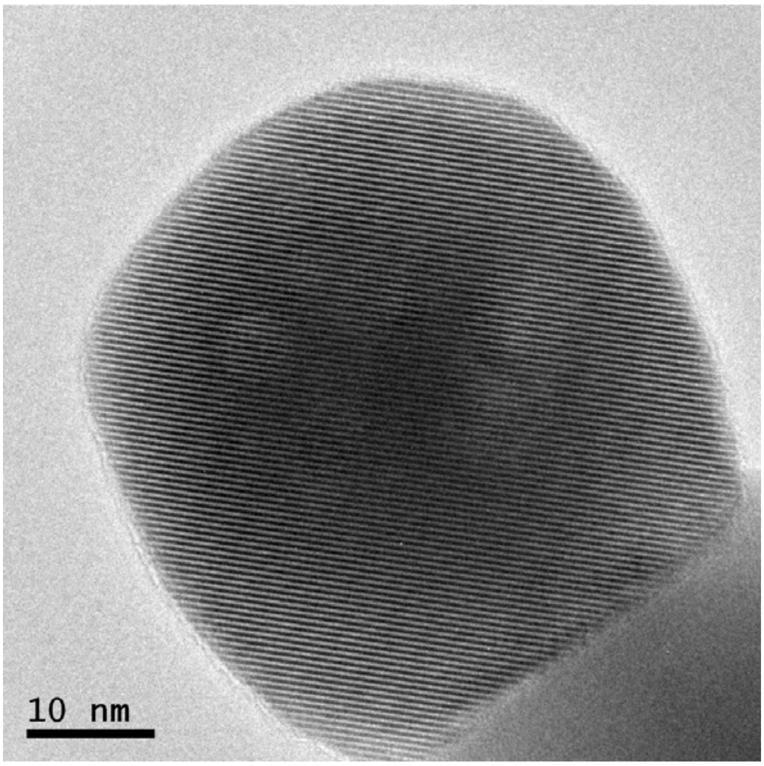

Figure 7: HRTEM image of crystalline Y_2O_3 prepared under accelerated electrons irradiation.

9. Aluminium oxide

Aluminium oxide is used in various industrial applications such as protective coatings, soft abrasives, refractories, membranes, ceramic materials, etc. In recent decades the substantial attention has been devoted to study of organized nanoporous alumina, due to its thermal and chemical stability, adsorption capability and catalytic activity. Moreover the metastable forms of alumunium oxide (transition alumina) may be possibly used in other special applications such as thermometric gas sensors, dosimeters or precursors for oxide composites possessing promising luminescent, thermoluminescent and scintillation properties.

We studied preparation of aluminium oxide and different transient phases of alumina using radiation and photochemical method. For radiation experiments, aqueous solutions of aluminium chloride or nitrate were used, with alkaline formate and/or hydrogen peroxide added. During irradiation, the pH value of solutions containing H_2O_2 increases. Irradiation led to the formation of finely dispersed amorphous colourless gel containig probably mixture of hydrated aluminium hydroxides or oxohydroxides. Subsequent heat treatment at temperatures 500-1200°C in air or under vacuum leads, depending on the temperature, to the various crystalline modifications of alumina (pseudoboehmite, γ-, θ- and α-Al_2O_3) with different textural and structural parameters.

10. Yttrium-aluminium garnet

Yttrium aluminium garnet $Y_3Al_5O_{12}$ (YAG) is synthetic crystalline material with cubic structure. Powder YAG may be used for preparation of transparent optical ceramics. When doped with foreign ions (e.g. lanthanides), such ceramics may serve as cheaper alternative to single crystalline YAG for applications in solid-state lasers, as phosphor in cathode ray tubes, in radiation dosimetry or as a scintillating material also in an optical ceramic form.

In irradiation experiments, two aqueous systems were studied with components mixed at molar ratios corresponding to YAG stoichiometry:

Aqueous solution containing aluminium choride, yttrium nitrate and potassium formate.

Aqueous solution containing aluminium nitrate, yttrium nitrate and potassium formate.

It was found, that under either of both types of used irradiation, solid phase is quantitatively formed. In this respect, no differences were observed between ionizing and UV radiation. After irradiation, the finely dispersed solid phase was separated, dried and thermally treated at various temperatures. No differences were observed in the color of filtered and dried solid phase, either. After calcination for 1h at 1000°C, the XRPD spectra of materials formed under both UV and accelerated electrons irradiation show pure YAG phase with well developed crystals (example in Fig. 8).

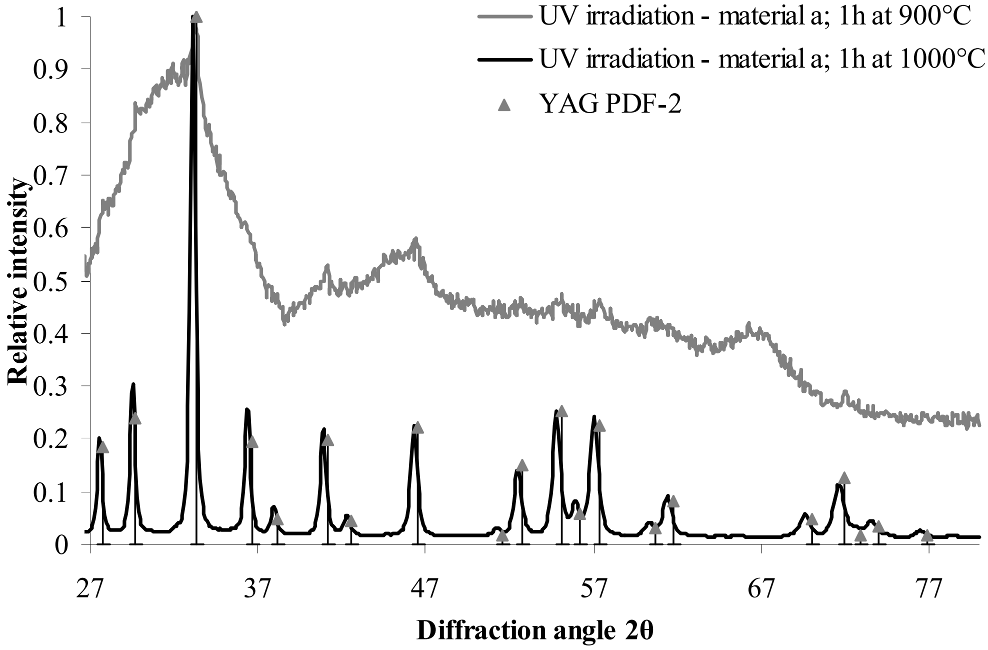

Figure 8: XRPD analysis of YAG formed under UV irradiation and calcinated at 900 or 1000 °C.

However, XRPD spectra of materials prepared under accelerated electrons irradiation and calcinated at higher temperatures show some low intensity lines corresponding to yttrium oxide; at even higher calcination temperatures, also lines of alpha – aluminium oxide were observed. Under the same conditions, samples prepared under UV irradiation show pure YAG phase only. XRPD results thus indicate that yttrium and aluminium based components of formed solid phase blend much better under UV irradiation than under electron irradiation. When compared to the UV irradiation, the deposition of energy under accelerated electrons irradiation is very fast and highly non-uniform. Used linear electron accelerator implants the energy to the matter in short pulses (~ 3 μs), followed by comparatively long relaxation time (2 ms). Thus, the formed solid phase may feature non-uniformities with regards to both major components. TEM images show that prepared YAG consists of aggregates formed by smaller (probably single crystalline) particles with ~50 nm size; (see example in Fig 9).

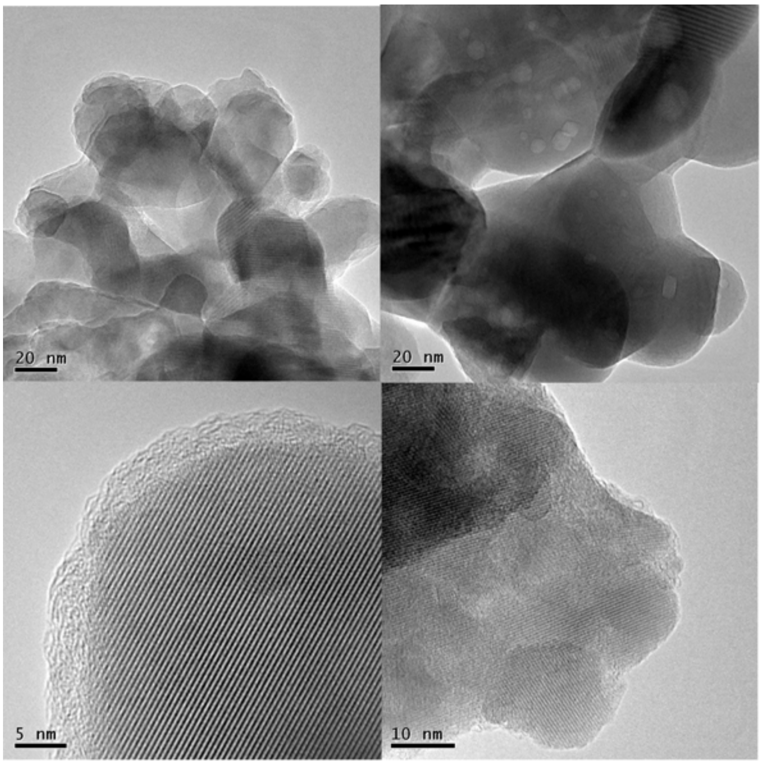

Figure 9: HRTEM images of YAG phase calcinated at 1000°C. Upper and lower left – formed under UV irradiation; upper and lower right - formed under accelerated electrons irradiation.

Example of radioluminescence (RL) spectra of prepared materials is shown in Fig. 10. The dominating broad band at about 530 nm can be ascribed to Ce^{3+} center (Weber 1973; Bachmann et al. 2009) which is due to Ce^{3+} impurity in raw materials (used precursor yttrium nitrate contains 100 ppm of CeO_2 and 300 ppm of La_2O_3). The band in UV area can be most probably ascribed to a defect-trapped exciton; e.g. the La and Sc related emissions in YAG lattice occur in 4-5 eV region (Murk et al. 1995) and emission due to antisite defects or vacancies are also reported in UV region (Zorenko et al. 2005). The line emissions around

310 nm and 670-720 nm can be ascribed to Gd^{3+} and unidentified rare earth impurity, respectively. It was observed, that the samples prepared under UV irradiation show the highest RL intensity. It can be taken as a measure of scintillation efficiency exceeding several times that of $Bi_4Ge_3O_{12}$ (BGO) powder reference scintillator sample. This indicates very good quality of YAG material containing low concentration of quenching sites of any kind. The samples prepared under electron irradiation show considerably lower RL intensity which can be due to the previously mentioned structural non-uniformities arising in this kind of manufacturing process and resulting in high concentration of defects at atomistic scale.

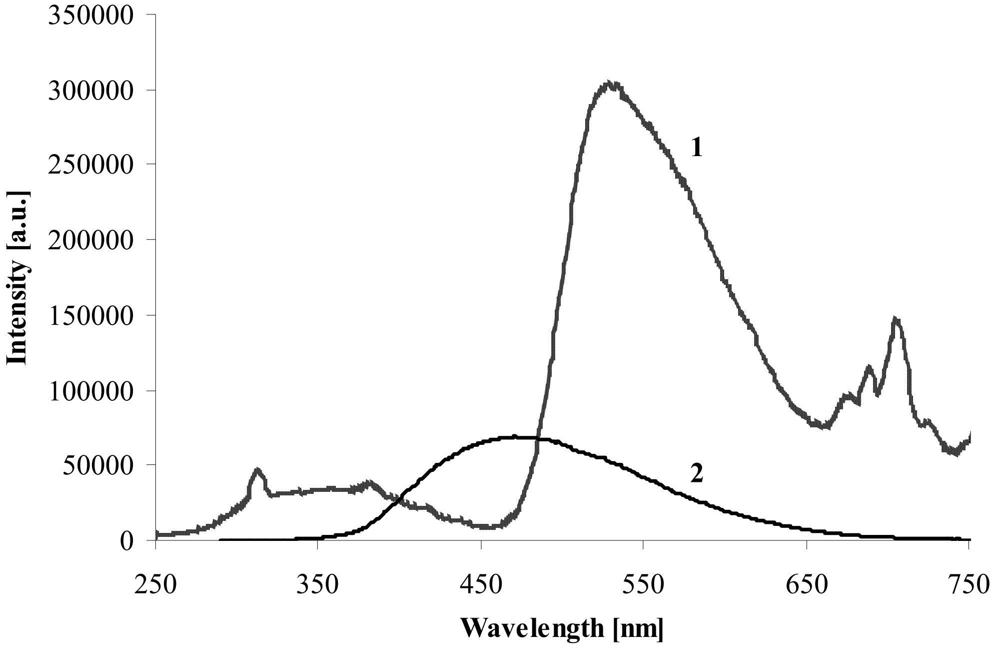

Figure 10: radioluminescence spectra of YAG prepared under UV irradiation and calcinated at 1300 °C (1), compared to BGO (2).

11. Conclusions

Convenient simple method for preparation of crystalline or amorphous (nano)powder materials with interesting properties was discussed in this lecture. The method is based on irradiation of aqueous solutions containing precursors (metal salts) with ionizing or non-ionizing radiation. Presence of organic compounds scavenging OH radicals and/or protecting small particles of metal/oxide from agglomeration is also needed to achieve high quality nanocrystals when using this technology. Prepared materials have high chemical purity and narrow distribution of particles size.

Generally, both types of radiation yield materials with comparable properties and structural characteristics, but in some cases, UV-radiation seems to be more convenient for materials preparation. This is especially the case for YAG preparation.

Among discussed compounds, silver/copper metals and cuprous/zinc oxides were prepared directly via irradiation. For preparation of nickel, yttrium and aluminium oxides, and yttrium-aluminium garnet, additional heat treatment of amorphous solid phase was necessary.

12. References

An Y-J, Jeong S-W, Carraway ER (2001) Water Res 35:3276-3279.

Arena V (1971) Ionizing radiation and life: an introduction to radiation biology and biological radiotracer methods. Mosby, Saint Louis.

Azrague K, Bonnefille E, Pradines V, Pimienta V, Oliveros E, Maurette M-T, Benoit-Marquié F (2005) Photochem Photobiol Sci 4:406-408.

Bachmann V, Ronda C, Meijerink A (2009) Chem Mater 21:2077-2084.

Belloni J, Mostafavi M, Remita H, Marignier J-L, Delcourt M-O (1998) New J Chem 1239-1255.

Bourret-Courchesne ED, Derenzo SE, Weber MJ (2009) Nucl Instrum Meth A 601:358-363.

Buono-Core GE, Cabello G, Klahn AH, Del Rio R, Hill RH (2006) J Non-Cryst Solids 352:4088-4092.

Buxton GV, Greenstock CL, Helman WP, Ross AB (1988) J Phys Chem Ref Data 17:513-886.

Giuffrida S, Constanzo LL, Ventimiglia G, Bongiorno C (2008) J Nanopart Res 10:1183-1192.

Hu Y, Chen J, Xue X, Li T, Xie Y (2005) Inorg Chem 44:7280-7282.

Huang G, Zhanglian H, Shizhu Z, Pengyue Z, Xianping F (2006) J Rare Earth 24: 47-50.

Kapoor S, Palit DK, Mukherjee T (2002) Chem Phys Lett 355:383-387.

Kumar M, Kapoor S, Gopinathan C (1999) Radiat Phys Chem 54:39-44.

Loginov AV, Gorbunova VV, Boitsova TB (2002) J Nanopart Res 4:193-205.

Mallick K, Witcomb MJ, Scurrell MS (2004) J Mater Sci 39:4459-4463.

Muresan L, Popovici E-J, Grecu R, Tudoran LB (2009) J Alloy Compd 471:421-7.

Murk V, Yaroshevich N (1995) J Phys - Condens Mat 7:5857-5864.

Nikonorova GK, Shubin VN, Brusentseva SA, Dolin PI (1976) Vodn Resur 3:149–155.

Ohshima E, Ogino H, Niikura I, Maeda K, Sato M, Ito M, Fukuda T (2004) J Cryst Growth 260:166-170.

Rath MC, Sunitha Y, Ghosh HN, Sarkar SK, Mukherjee T (2009) Radiat Phys Chem 78:77-80.

Sebok D, Szabo T, Dekany I (2009) Appl Surf Sci 255:6953-6962.

Shvalagin VV, Stroyuk AL, Kuchmii SY (2004) Theor Exp Chem 40:378-382.

Shvalagin VV, Stroyuk AL, Kuchmii SY (2007) J Nanopart Res 9:427-440.

Sukhov NL, Ershov NB, Mikhalko K, Gordeev AV (1997) Russ Chem Bull 46:197–199.

Sun M, Hao W, Wang C, Wang T (2007) Chem Phys Lett 443:342-346.
Tak Y, Yong K (2008) J Phys Chem C 112:74-79.
Weber MJ (1973) Solid State Commun 12:741-744.
Wilkinson J, Ucer KB, Williams RT (2004) Radiat Meas 38:501-505.
Zhou R, Wu X, Hao X, Zhou F, Li H, Rao W (2008) Nucl Instrum Meth B 266:599-603.
Zhu Y, Qian Y, Zhang M, Chen Z, Xu D (1994) Mater Res Bull 29:377-383.
Zorenko Y, Gorbenko V, Konstankevych I, Voloshinovskii A, Stryganyuk G, Mikhailin V, Kolobanov V, Spassky D (2005) J Lumin 114:85-94.

13. Ing. Václav Čuba, Ph.D. – curriculum vitae

Date and place of birth:
03/02/1976 in Prague, Czech Republic

Undergraduate study:
1994 – 1999: study at FNSPE CTU in Prague, MSc in nuclear chemical engineering.

Postgraduate study:
1999 – 2003: PhD study at FNSPE CTU in Prague; Ph.D. in nuclear chemistry obtained in 2003.

Employment:
Since 2003 – assistant and research professor at CRRC and FNSPE CTU in Prague.

Fields of interest:
Applied radiation chemistry and photochemistry, radiation processing.

Teaching activities:
Active in teaching since 2004. 2 regular obligatory courses (1 in bachelor, 1 in master programme), 2 practical exercises (bachelor programme) and 2 laboratory exercises (master programme). In 2006 introduced new obligatory course Radiation methods in biology and medicine for specialization Nuclear chemistry in biology and medicine. Since 2010 member of committee for state examinations in bachelor programme.

Scientific/research activities:
Coauthor of tens of original research papers published in international journals or presented in international conferences, coauthor of two chapters in book and numerous peer-reviewed technical reports. Member of editorial board of Journal of Radioanalytical and Nuclear Chemistry, reviewer for four international journals (Advances in Colloid and Interface Science, Material Science and Engineering B, Journal of Radioanalytical and Nuclear Chemistry, Journal of Nanoparticle Research), opponent of grants provided by Ministry of Education, Youth and Sports.

Supervisor of Ph.D, diploma and bachelor theses. Team member of numerous domestic and international grants (4 GACR grants, 1 GA AS CR grant, 1 /8th EU FP, 1 DAAD grant, 3 MSM grants), scientific and administrative supervisor of 5 domestic grants (including 2 GACR grants and 1 MSM grant as both applicant and joint applicant).